Open Ceramics 21 (2025) 100723

Contents lists available at ScienceDirect

Open Ceramics

journal homepage: www.sciencedirect.com/journal/open-ceramics

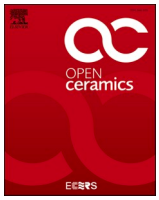

Microstructure and thermal-mechanical evolution of high-entropy pyrochlore ($A_2B_2O_7$) with dual crystalline phase

Kun Yang [a], Minghao Zhao [a], Huan Li [b,*], Chengying Bai [c]

[a] Department of Nuclear Science and Technology, Nanjing University of Aeronautics and Astronautics, Nanjing 210016, PR China
[b] Xi'an Rare Metal Materials Institute Co. Ltd., Xi'an, 710016, PR China
[c] Department of Materials Science and Chemical Engineering, Harbin Engineering University, Harbin, 150006, China

ARTICLE INFO

Keywords:
Pyrochlore
Dual-phase
High-entropy
Irradiation
Thermal conductivity

ABSTRACT

Chemical complex solid solutions with dual-phases were successfully synthesized through solid-state reaction with its thermal-mechanical behavior subjected to proton irradiation were characterized. The dual-phase structural solid solutions demonstrate reduced thermal conductivity and enhanced mechanical performance, which can be associated with its chemical disorder and lattice distortion. Radiation hardening can be observed for the sample pellets with slight surface amorphization occurring, resulting in a Ti-enriched alteration layer covered on the surface.

1. Introduction

Recently, the extraordinary thermal, mechanical, and radiation resistance of the pyrochlore or fluorite multicomponent solid solutions $A_2B_2O_7$ has raised intensive research worldwide, especially in the typical fields of environmental barrier coating (EBC), catalyst for hydrogen production and nuclear waste form[1]. Previous research by Guo et al.[2] suggested that the cationic ionic radii ratio is the critical parameter in judging the radiation resistance for high-entropy pyrochlore solid solutions. Chemical complex solid solutions with highly tunable crystalline structures can feasibly control the cationic ionic radii and simultaneously alter its crystalline structure due to the potential introduced large lattice distortion. The significant large lattice distortion induced by large ionic differences within the cationic elements further leads to the dual-phase structure, which might extend superior thermal, radiation, and corrosion resistance[3,4]. Thermal conductivity was recognized to have a strong negative correlation with size disorder, acting as an ideal predictor for thermal conductivity [5]. Therefore, it is reasonable to assume that large-size disorder coupled with dual-phase structure can affect the key material parameters as well. In the current study, dual-phase $A_2B_2O_7$ solid solutions were successfully synthesized to align with the large-size disorder by introducing cationic elements with large ionic radii differences into the A-site, while the thermal, mechanical property and its microstructure evolution of the as-synthesized dual-phase solid solutions were characterized before and post proton irradiation.

2. Materials and methods

Equally amount of rare earth oxides (La_2O_3, Nd_2O_3, Sm_2O_3, Eu_2O_3, Gd_2O_3, Dy_2O_3, Tm_2O_3, and TiO_2) were dried in an oven at 300 °C for 2 hours following by ball-milling for 24 hours with a rotating speed of 500 r/min (Fig. 1(a)). The high-temperature consolidation can be achieved by ultra-fast hot-pressing at 1250 °C and 50 MPa with a thermal holding time of 30 minutes, the theoretical density of the samples are greater than 90%. The proton irradiation was carried out at the Institute of Modern Physics, Chinese Academy of Sciences (Lanzhou, China) with proton energy of 1.52 MeV at room temperature, achieving a final fluence of 5×10^{18} cm^{-2}. The microstructure evolution of the as-consolidated sample coupons before and post proton irradiation can be characterized by Scanning Electron Microscopy (SEM) (TESCAN LYRA3 GM), Scanning Transmission Electron Microscopy (STEM) (Spectra 300 (S)TEM) equipped with an Energy Dispersive Spectroscopy (EDS). The crystalline phase structure and localized chemical bonding environment were determined by X-ray Diffraction (XRD) (PAN analytical) and Confocal Raman Spectroscopy (HORIBA HR Evolution). The thermal conductivity can be calculated by measuring the thermal diffusivity of the sample pellets with a laser thermal conductivity meter (NETZCH 100) at elevated temperatures from 25 °C to 900 °C[6]. The mechanical property of the surface alteration layer post-irradiation can

* Corresponding author.
E-mail address: lihuan@nuaa.edu.cn (H. Li).

https://doi.org/10.1016/j.oceram.2024.100723
Received 12 September 2024; Received in revised form 12 November 2024; Accepted 6 December 2024
Available online 7 December 2024

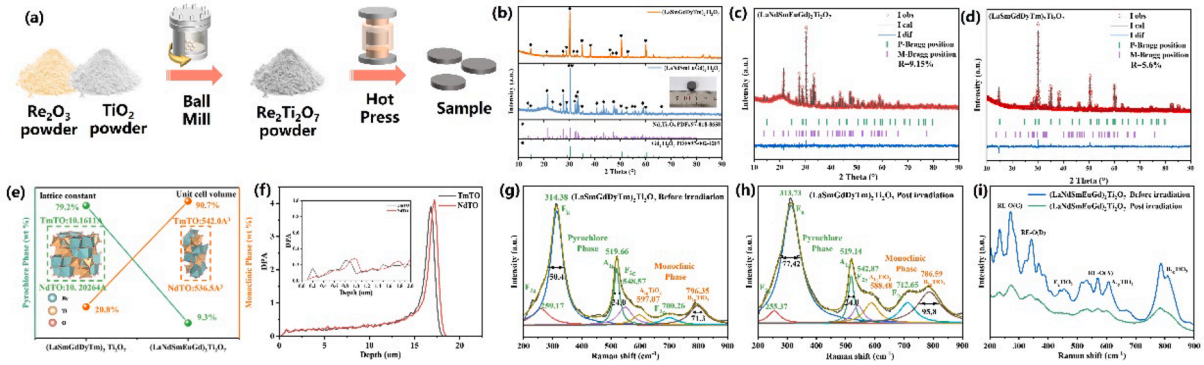

Fig. 1. (a) Solid-state sintering process for the Chemical complex solid solution (b) XRD profiles for the $(La_{0.2}Sm_{0.2}Gd_{0.2}Dy_{0.2}Tm_{0.2})_2Ti_2O_7$ (TmTO) and $(La_{0.2}Nd_{0.2}Sm_{0.2}Eu_{0.2}Gd_{0.2})_2Ti_2O_7$ (NdTO) (c-d) XRD Peak Refinement Results (e) Semi-quantitative analysis of the sample pellets based on Rietveld peak refinement (f) Calculated displacement damage of TmTO and NdTO at a fluence of 5×10^{18} cm^{-2} (g-i) Raman spectra of the sample pellets before and post proton irradiation.

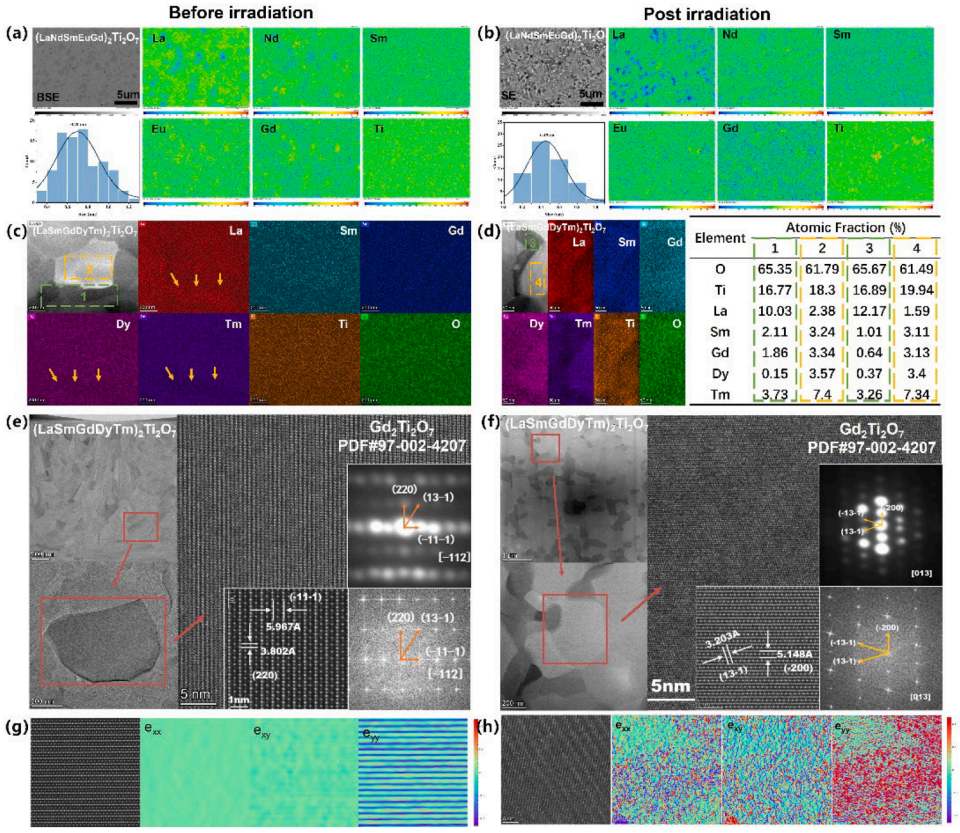

Fig. 2. (a,b)EPMA mappings of the sample pellets before and post proton irradiation; (c-f) STEM-EDS analysis of the sample pellet; (g,h) geometrical phase analysis of the sample pellet.

be further determined by nano-indentation and micro-indentation (Vicker hardness).

3. Results and discussion

The XRD profiles of the as-fabricated sample pellet can be seen in Fig. 1(b), which indicates the coexistence of characteristic peaks of 38° (331) and 42° (511) for pyrochlore, 21° and 33° for monolithic structure, suggesting the dual-phases property. The XRD refinement outcomes for the two sample pellets are depicted in Fig. 1(c, d). The semi-quantitative phase analysis suggests pyrochlore and monolithic phases composed of 79.2% and 20.8% for $(La_{0.2}Sm_{0.2}Gd_{0.2}Dy_{0.2}Tm_{0.2})_2Ti_2O_7$ (TmTO), and 9.3% and 90.7% for $(La_{0.2}Nd_{0.2}Sm_{0.2}Eu_{0.2}Gd_{0.2})_2Ti_2O_7$ (NdTO), respectively. The distinguishable phase compositions suggest that doping large cationic ionic radii elements accelerates the phase transition to monolithic (Fig. 1(e)). The proton irradiation induces localized chemical bonding distortion as well as slightly surface amorphilization since the E_g and F_{2g} Raman peaks belongs to pyrochlore phase shift towards lower angle with the peak became wider and the peak intensity became weaker for both sample pellets.

The surface roughness significantly increases with partial grain defoliation observed for the sample surface post-proton irradiation. The surface post-proton irradiation featured a Ti-enriched layer, which can be attributed to the surface elemental reorganization. The d-spacing towards different crystalline planes was determined as 3.802Å and 5.967Å, consistent with the crystalline planes of (220) and (-11–1) in

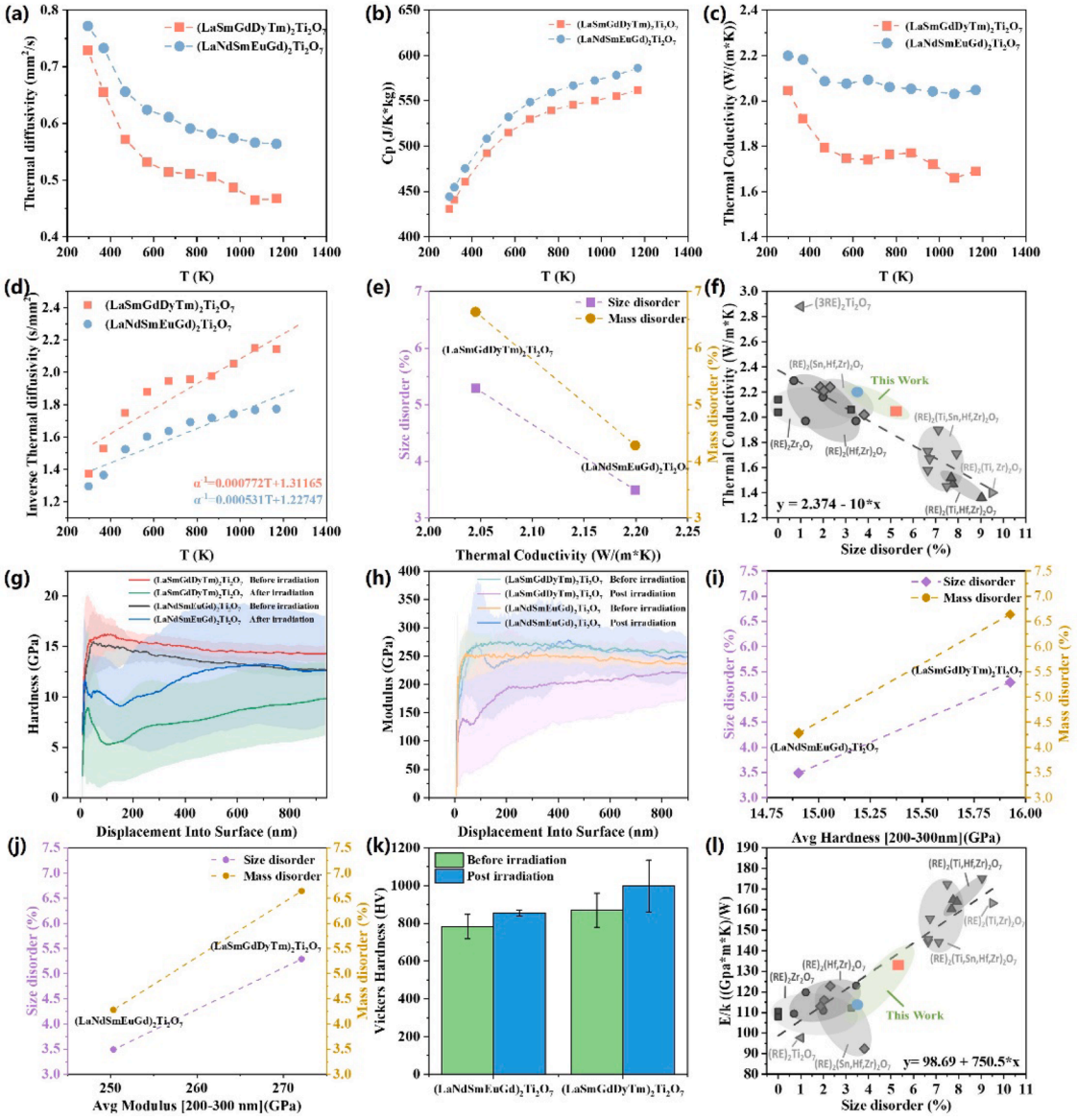

Fig. 3. (a-c) thermal diffusivity, capacity, and thermal conductivity (d) inverse thermal diffusivity (e) chemical disorder VS thermal conductivity at 298K (f) comparison of thermal conductivity with literature; (g) nano-indentation hardness (h) Young's Modulus; nano indentation VS chemical disorder at 200–300 nanometers (i) nano-indentation hardness (j) Young's Modulus; (k) Vickers hardness (l) comparison of the ratio of Young's modulus to thermal conductivity (E/k) with literatures.

$Gd_2Ti_2O_7$ before irradiation. The proton irradiation-induced lattice shrank was further confirmed by the reduction of the lattice constant. The significant lattice distortion induced by the formation of a chemical complex solid solution can be evidenced by the geometric phase analysis (GPA), which indicates an increase in the stress distribution post-proton irradiation, especially on the (220) crystalline plane (Fig. 2g, h).

Results indicate the relatively lower thermal conductivity of $(La_{0.2}Sm_{0.2}Gd_{0.2}Dy_{0.2}Tm_{0.2})_2Ti_2O_7$ (TmTO) with large lattice distortion derived from the large size and mass disorder (Fig. 3(e)). The thermal conductivities of the two sample pellets at 298K are 2.05 $W{\cdot}m^{-1}{\cdot}K^{-1}$and 2.2 $W{\cdot}m^{-1}{\cdot}K^{-1}$, separately, lower than the $(3REE)_2Ti_2O_7$, while the thermal conductivity of the dual-phase solid solutions exhibit negative correlation to size disorder (Fig. 3(f))[5]. The surface nano-indentation (200–300 nm in depth) hardness faces decrease for both sample pellets post proton irradiation, which can be attributed to the potential surface amorphization caused by the irradiation. The nano-indentation hardness, as well as Young's Modulus increases with the chemical disorder (Fig. 3i-j). On the other hand, the bulk Vicker hardness increases post proton irradiation for both sample pellets, contradicting the result from nano-indentation, which can be attributed to the radiation hardening effect, although the top surface occurred with a certain level of amorphization. Specifically, the Vickers hardness post-irradiation increases with a level of about 14.78% and 9.08% for $(La_{0.2}Sm_{0.2}Gd_{0.2}Dy_{0.2}Tm_{0.2})_2Ti_2O_7$ (TmTO) and $(La_{0.2}Nd_{0.2}Sm_{0.2}Eu_{0.2}Gd_{0.2})_2Ti_2O_7$ (NdTO), separately. As a result, the ratio of Young's modulus to thermal conductivity (E/k) for the two sample pellets are 133.1 $GPa{\cdot}m{\cdot}K{\cdot}W^{-1}$ and 113.8 $GPa{\cdot}m{\cdot}K{\cdot}W^{-1}$, separately, both of which are higher than the $(3REE)_2Ti_2O_7$, while the E/k values of the dual-phase solid solutions exhibit positive correlation to size disorder (Fig. 3(l))[5].

4. Conclusion

The pyrochlore and monolithic dual-phase chemical complex rare earth $A_2Ti_2O_7$ solid solutions demonstrate reduced thermal conductivity of 2.05 $W{\cdot}m^{-1}{\cdot}K^{-1}$ and 2.2 $W{\cdot}m^{-1}{\cdot}K^{-1}$, while the proton irradiation induces radiation hardening with bulk Vicker hardness increase for

14.78% and 9.08%, respectively. The as-synthesized sample pellets demonstrate robust proton radiation resistance with enhanced thermal and mechanical behavior compared to single-phase Ti-pyrochlore solid solutions, with slightly surface reorganization occurred. The current study demonstrates a novel materials design strategy with improved thermal, mechanical, and radiation resistance, which is promising to be used in extremes of advanced energy systems.

CRediT authorship contribution statement

Kun Yang: Investigation. **Minghao Zhao:** Data curation. **Huan Li:** Investigation. **Chengying Bai:** Methodology.

Declaration of competing interest

The authors declare that they have no known competing financial interests or personal relationships that could have appeared to influence the work reported in this paper.

Acknowledgement

The authors would like to express appreciation for financial support from the National Natural Science Foundation of China (No. 37244600).

References

[1] M.A. Subramanian, G. Aravamudan, G.V. Subba Rao, Oxide pyrochlores — a review, Prog. Solid State Chem. 15 (1983), https://doi.org/10.1016/0079-6786(83)90001-8.

[2] H. Guo, K. Zhang, Y. Li, Heavy-ion irradiation effects of high-entropy A2Ti2O7 pyrochlore with multi-elements at a site, Ceram. Int. 50 (2024) 21859–21868, https://doi.org/10.1016/j.ceramint.2024.03.298.

[3] G. Chen, C. Li, H. Jia, Y. Zhang, B. Gong, X. Li, T. Liu, K. Chen, A novel approach for the composition design of high-entropy fluorite oxides with low thermal conductivity, J. Adv. Ceram. (2024), https://doi.org/10.26599/JAC.2024.9220942.

[4] J. Zhu, X. Meng, P. Zhang, Z. Li, J. Xu, M.J. Reece, F. Gao, Dual-phase rare-earth-zirconate high-entropy ceramics with glass-like thermal conductivity, J. Eur. Ceram. Soc. 41 (2021) 2861–2869, https://doi.org/10.1016/j.jeurceramsoc.2020.11.047.

[5] A.J. Wright, Q. Wang, S.-T. Ko, K.M. Chung, R. Chen, J. Luo, Size disorder as a descriptor for predicting reduced thermal conductivity in medium- and high-entropy pyrochlore oxides, Scr. Mater. 181 (2020) 76–81, https://doi.org/10.1016/j.scriptamat.2020.02.011.

[6] Z. Chen, Y. Huang, Z. Zhang, W. Zheng, X. Song, Y. Niu, Y. Zeng, Investigation of improving the thermophysical properties and corrosion resistance of RE_2SiO_5 /$RE_2Si_2O_7$ multiphase silicates by component design with RE doping, J. Adv. Ceram. 13 (2024) 842–860, https://doi.org/10.26599/JAC.2024.9220903.